

NAVIGATION STRATEGIES FOR MULTIPLE AUTONOMOUS MOBILE ROBOTS
MOVING IN FORMATION

P.K.C. Wang

Department of Electrical Engineering
University of California
Los Angeles, California 90024
U.S.A.

Abstract: The problem of deriving navigation strategies for a fleet of autonomous mobile robots moving in formation is considered. Here each robot is represented by a particle with a spherical effective spatial domain and a specified cone of visibility. The global motion of each robot in the world space is described by the equations of motion of the robot's center of mass. First, methods for formation generation are discussed. Then, simple navigation strategies for robots moving in formation are derived. A sufficient condition for the stability of a desired formation pattern for a fleet of robots each equipped with the navigation strategy based on nearest neighbor tracking is developed. The dynamic behavior of robot fleets consisting of three or more robots moving in formation in a plane is studied by means of computer simulation.

1. INTRODUCTION

In space and underwater exploration, it is of interest to use fleets of autonomous mobile robots in place of humans. Due to uncertainties in the environment, it is advantageous for the robots to move in a prescribed formation such that each robot is visible from any other robot, and they are separated from each other with a prescribed distance at all times. A fleet of autonomous mobile robots may also be used in factories with unstructured environment. These robots may move in formation from one place to another in the factory to perform certain tasks. Their path is determined by a designated fleet leader. In both cases, the following basic questions should be considered:

- (i) How does one derive effective implementable navigation strategies for a fleet of autonomous robots moving in formation?
- (ii) Given a desired formation pattern for a fleet of robots with a given navigation strategy for each robot, how do the robots interact dynamically in the presence of perturbations in the robot motions?

In nature, one often observe that large schools of fish or flocks of birds are capable of maneuvering at high speeds while maintaining the prescribed formation patterns with precision. An understanding of their navigation methods for moving in formation would be helpful in providing answers to the foregoing questions.

In this paper, we consider the problem of deriving simple strategies for navigating a fleet of autonomous robots in formation, and study the interaction dynamics of these robots equipped with the derived navigation strategies. This work is in the spirit of our earlier studies [1], [2] on the interaction dynamics of multiple autonomous mobile robots in which each robot is represented by a particle with a spherical effective spatial domain and a specified cone of visibility. In contradistinction with most of the existing works on autonomous mobile robots in which the emphasis is on algorithms for path planning in the presence of obstacles [3]-[6], we focus our attention on the global dynamic behavior of a fleet of mobile robots consisting of a few to possibly a few thousand robots moving in formation.

In the development of this paper, we begin with the basic equations describing the global motion of the robots. Then various types of formation are introduced.

This is followed by the derivation of various navigation strategies for robots moving in formation. Then, a sufficient condition for the stability of the formation pattern for a fleet of robots each equipped with a particular type of navigation strategy is obtained. Finally, the dynamic behavior of robot fleets consisting of three or more robots moving in formation in a plane is studied by means of computer simulation.

2. PRELIMINARIES

Let R^n denote the n -dimensional real Euclidean space. The world space is taken to be R^3 with its origin coinciding with the inertial frame whose coordinate system is defined by a fixed orthonormal basis $\mathcal{B}_0 = \{e_x, e_y, e_z\}$. The representation of a point r in the world space with respect to \mathcal{B}_0 is given by (x, y, z) . The inner product between r and $r' \in R^3$ is denoted by $\langle r, r' \rangle = xx' + yy' + zz'$ and the Euclidean norm of r by $\|r\|$. The closed ball of radius ρ centered at r_0 is denoted by $S_\rho(r_0) = \{r \in R^3: \|r - r_0\| \leq \rho\}$, and its boundary by $\partial S_\rho(r_0)$.

We consider a fleet of N mobile robots. The position of the mass center of the i -th robot at time t is specified by $r_i(t) = x_i(t)e_x + y_i(t)e_y + z_i(t)e_z$. The effective spatial domain occupied by the i -th robot at time t is taken to be $\Sigma_i(t) = S_{\rho_i}(r_i(t))$, where ρ_i is a specified radius. Physically, the sphere $\partial S_{\rho_i}(r_i(t))$ contains the robot's body such that its penetration by other robots is considered as a collision. More precisely, the i -th and j -th robots are said to be colliding at time t , if $\Sigma_i(t)$ and $\Sigma_j(t)$ have common interior points. As in [1], we assume that each robot has a vision system whose cone of visibility at time t

is defined by $\Gamma_i(t) = S_{\rho_{vi}}(r_i(t)) \cap C_{h_i(t)}(r_i(t), \phi_i)$,

where $C_{h_i(t)}(r_i(t), \phi_i)$ denotes the closed convex cone of revolution with its vertex at $r_i(t)$, aperture angle ϕ_i , and axis of revolution $h_i(t)$ defined by

$$C_{h_i(t)}(r_i(t), \phi_i) = \{r \in R^3: 0 \leq \cos^{-1}[\langle r - r_i(t), h_i(t) \rangle / (\|r - r_i(t)\| \|h_i(t)\|)] \leq \phi_i\}. \quad (1)$$

Usually, the vector $h_i(t)$ corresponds to the heading of the i -th robot. The visibility radius ρ_{vi} may be finite or infinite, and satisfies $\rho_{vi} > \rho_i$. The j -th robot is said to be completely visible (resp. visibly) from the i -th robot at time t , if $\Sigma_j(t) \subset \Gamma_i(t)$ (resp. $\Sigma_j(t) \cap \Gamma_i(t) \neq \emptyset$).

In this study, attention is focused on the global motion of each robot in the world space. The position and orientation of the arms and end-effectors are not considered here. To model the global robot dynamics,

each robot is taken as a point mass inside its spherical spatial domain. The equations of motion of the mass center of the i -th robot are assumed to be describable by

$$M_1 \ddot{\mathbf{r}}_1(t) + \nu_1 \dot{\mathbf{r}}_1(t) = \mathbf{F}_c^1(t), \quad (2)$$

where M_1 is the total mass; the overdot denotes differentiation with respect to time t ; and ν_1 is a non-negative friction coefficient. For underwater robots, the term $\nu_1 \dot{\mathbf{r}}_1(t)$ may correspond to the hydrodynamic drag; and for space robots, ν_1 may be set to zero. Here, the control force $\mathbf{F}_c^1 = f_{cx}^1 \mathbf{e}_x + f_{cy}^1 \mathbf{e}_y + f_{cz}^1 \mathbf{e}_z$ is assumed to be a piecewise continuous function of t taking its values in the compact control region:

$$\Omega_1 = \{\mathbf{F}_c^1 \in \mathbb{R}^3: |f_{cj}^1| \leq \bar{F}_c^1, j = x, y, z\}, \quad (3)$$

where \bar{F}_c^1 is a specified positive constant.

As in [1], we assume that the robots have no rigid-body rotation so that the axis of revolution $\mathbf{h}_1(t)$ associated with the cone of visibility $C_{h_1(t)}(\mathbf{r}_1(t), \phi_1)$

of the i -th robot remains aligned with the robot heading $\dot{\mathbf{r}}_1(t)$ at all times. Figure 1 shows the basic features of a mobile robot under consideration.

3. NAVIGATION STRATEGIES FOR MOVEMENT IN FORMATION

The movement of robots in formation can be achieved in a number of ways. We shall consider a few simple approaches.

3.1 Nearest-Neighbor Tracking: Here, a robot, say the first one, is designated as the fleet leader who specifies a reference motion for the fleet denoted by $\mathcal{R}_1 = \{\mathbf{r}_1(t), t \in \bar{I}_T\}$, where $\bar{I}_T = [0, T]$ is a given time interval. Let the desired motion for the second robot (follower) be specified by

$$\mathbf{d}_2(t) = \mathbf{r}_1(t) + \mathbf{q}_2(t), \quad (4)$$

where $\mathbf{q}_2 = \mathbf{q}_2(t)$ is a specified nonzero deviation vector defined for all $t \in \bar{I}_T$ and twice continuously differentiable on \bar{I}_T . Moreover, to avoid the possibility of a collision between the two robots, we impose the constraint that $\|\mathbf{q}_2(t)\| > \rho_1 + \rho_2$ for all $t \in \bar{I}_T$, where ρ_1 denotes the radius of the ball containing the i -th robot as mentioned earlier. The second robot tries to track the motion of the leader such that the norm of the tracking error vector

$$\mathbf{E}_2(t) \triangleq \mathbf{d}_2(t) - \mathbf{r}_2(t) \quad (5)$$

is within a specified bound.

The desired motion for the i -th robot, $i \geq 2$, can take on one of the following forms:

$$\mathbf{d}_i(t) = \mathbf{r}_{i-1}(t) + \mathbf{q}_i(t) \quad (6)$$

or

$$\mathbf{d}_i(t) = \mathbf{d}_{i-1}(t) + \mathbf{q}_i(t) = \mathbf{r}_1(t) + \sum_{k=2}^i \mathbf{q}_k(t), \quad (7)$$

where $\mathbf{q}_i = \mathbf{q}_i(t)$ is a specified deviation vector having properties similar to those of \mathbf{q}_2 . The i -th robot tries to navigate in such a way that the norm of the tracking error

$$\mathbf{E}_i(t) \triangleq \mathbf{d}_i(t) - \mathbf{r}_i(t) \quad (8)$$

is within a specified bound.

Evidently, for any fixed $t \in \bar{I}_T$, the point set $\mathcal{P}(t) =$

$\{\mathbf{r}_1(t), \mathbf{r}_1(t) + \mathbf{q}_2(t), \mathbf{r}_1(t) + \mathbf{q}_2(t) + \mathbf{q}_3(t), \dots, \mathbf{r}_1(t) + \sum_{k=2}^N \mathbf{q}_k(t)\}$ defines a formation pattern at time t in the world space. In the simplest case where $\mathbf{q}_i, i = 2, \dots, N$ are constant nonzero vectors, $\mathcal{P}(t)$ is generated by time-invariant translations of the reference motion \mathcal{R}_1 specified by the fleet leader. A more complicated example is given by $\mathbf{r}_1(t) = v_{10} t \mathbf{e}_z$; $\mathbf{q}_i(t) = \mu_i \cos(\omega_i t) \mathbf{e}_x + \mu_i \sin(\omega_i t) \mathbf{e}_y + v_{i0} t \mathbf{e}_z, i = 2, \dots, N$, where $v_{i0}, i=1, \dots, N$; ω_i and $\mu_i, i = 2, \dots, N$ are specified positive constants such that $\mu_{i+1} > \mu_i, i = 2, \dots, N$. In this case,

as time t varies over \bar{I}_T , the formation pattern $\mathcal{P}(t)$ sweeps out a set of concentric helixes rotating about the uniform motion of the leader along the z -axis.

In the case where $\mathbf{d}_i(t)$ is defined by (6), the motion of the $(i-1)$ -th robot is taken as the reference motion for the i -th robot. Thus, if any robot fails to converge to its desired motion, it would be impossible for the fleet to achieve the desired formation pattern. However, this form of $\mathbf{d}_i(t)$ has the advantage that

collisions between the i -th and $(i-1)$ -th robots are less likely to occur, since the i -th robot tries to maintain a specified deviation from the $(i-1)$ -th robot at all times. When $\mathbf{d}_i(t)$ is defined by (7), each follower robot tries to achieve its desired motion without monitoring the motion of its previous neighbor. Thus, a collision could occur under abnormal conditions.

In more general situations, the deviation vectors $\mathbf{q}_i(t)$ could depend on the states of the i -th or the $(i-1)$ -th robot at time t . For example, if we set $\mathbf{q}_i(t) = -\delta_i \dot{\mathbf{r}}_{i-1}(t) / \|\dot{\mathbf{r}}_{i-1}(t)\|$, where δ_i is a given positive constant, then the i -th robot tries to move directly behind the $(i-1)$ -th robot at δ_i distance away. We may also consider the case where there are more than one follower robots which track the reference motion of the fleet provided by the fleet leader. This leads to fleet formation patterns with many branches as illustrated in Fig. 2. Now, consider the following differential equation for the tracking error \mathbf{E}_i of the i -th robot defined in (8):

$$M_1 \ddot{\mathbf{E}}_i(t) + \nu_1 \dot{\mathbf{E}}_i(t) = M_1 \mathbf{g}_i(t) - \mathbf{F}_c^i(t), \quad (9)$$

where $\mathbf{g}_i(t)$ is given by

$$\mathbf{g}_i(t) = \left(\frac{\nu_1}{M_1} - \frac{\nu_{i-1}}{M_{i-1}} \right) \dot{\mathbf{r}}_{i-1}(t) + \frac{1}{M_1} \left(\ddot{\mathbf{q}}_i(t) + \nu_1 \dot{\mathbf{q}}_i(t) \right) + \mathbf{F}_c^{i-1}(t) / M_{i-1} \quad (10)$$

when $\mathbf{d}_i(t)$ is defined by (6); and

$$\mathbf{g}_i(t) = \ddot{\mathbf{d}}_i(t) + \frac{\nu_1}{M_1} \dot{\mathbf{d}}_i(t) \quad (11)$$

when $\mathbf{d}_i(t)$ is defined by (7).

Assuming that the visibility radius ρ_{v1} and the aperture angle ϕ_1 of the visibility cone of the follower robots are sufficiently large so that the $(i-1)$ -th robot

is visible from the i -th robot for all $t \in \bar{I}_T$, then a simple navigation strategy for the i -th follower robot with control region $\Omega_i = R^3$ is given by

$$F_c^i(t) = M_i g_i(t) + K_{11} E_i(t) + K_{12} \dot{E}_i(t), \quad (12)$$

where K_{11} and K_{12} are positive feedback gains. In this case, the differential equation for the tracking error E_i , $2 \leq i \leq N$, reduces to

$$M_i \ddot{E}_i(t) + (v_i + K_{12}) \dot{E}_i(t) + K_{11} E_i(t) = 0. \quad (13)$$

Evidently, assuming no collisions, $E_i(t) \rightarrow 0$ as $t \rightarrow \infty$. When $d_i(t)$ is defined by (6), $E_i(t) = r_{i-1}(t) - r_i(t) + q_i(t)$. In this case, the implementation of (12) requires a knowledge of the relative position and velocity between the i -th and $(i-1)$ -th robots, and also the navigation strategy of the $(i-1)$ -th robot. If communication between robots is permissible, then the position, velocity and navigation strategy of the $(i-1)$ -th robot could be transmitted to the i -th robot. Otherwise this information must be acquired by other means.

When the control region Ω_i is given by (3), the navigation strategy corresponding to (12) takes on the modified form:

$$F_c^i(t) = \bar{F}_c^i \text{SAT}\{(M_i g_i(t) + K_{11} E_i(t) + K_{12} \dot{E}_i(t))/\bar{F}_c^i\}, \quad (14)$$

$2 \leq i \leq N,$

where

$$\text{SAT}(w) \triangleq [\text{Sat}(w_1), \text{Sat}(w_2), \text{Sat}(w_3)]^T, \quad (15)$$

$$w = [w_1, w_2, w_3]^T,$$

and $\text{Sat}(\cdot)$ denotes the usual saturation function defined by

$$\text{Sat}(w) = \begin{cases} 1 & \text{if } w > 1, \\ w & \text{if } |w| \leq 1, \\ -1 & \text{if } w < -1. \end{cases} \quad (16)$$

In this case, the differential equation for E_i takes on the form:

$$M_i \ddot{E}_i(t) + v_i \dot{E}_i(t) = M_i g_i(t) - \bar{F}_c^i \text{SAT}\{(M_i g_i(t) + K_{11} E_i(t) + K_{12} \dot{E}_i(t))/\bar{F}_c^i\}, \quad 2 \leq i \leq N. \quad (17)$$

The behavior of the solutions of (17) will be analyzed later.

3.2 Multi-Neighbor Tracking: Consider a fleet of N mobile robots with $N \geq 3$. Let the first and the N -th robots be designated as leaders or guardians of the fleet. Their motions $\mathcal{R}_1 = \{r_1(t), t \in \bar{I}_T\}$ and $\mathcal{R}_N = \{r_N(t), t \in \bar{I}_T\}$ are taken as the reference motions for the fleet. Here, the desired position for the i -th follower robot ($1 \neq i, N$) at any time $t \in \bar{I}_T$ may be taken as the median of the positions of its nearest two neighbors at time t , i.e.

$$d_i(t) = (r_{i+1}(t) + r_{i-1}(t))/2. \quad (18)$$

The tracking error $E_i(t)$ for the i -th robot defined by (8) is described by the following differential equation:

$$M_i \ddot{E}_i(t) + v_i \dot{E}_i(t) = M_i \hat{g}_i(t) - F_c^i(t), \quad 2 \leq i \leq N-1, \quad (19)$$

where

$$\hat{g}_i(t) = \frac{1}{2} \left\{ \ddot{r}_{i+1}(t) + \ddot{r}_{i-1}(t) + \frac{v_i}{M_i} (\dot{r}_{i+1}(t) + \dot{r}_{i-1}(t)) \right\}, \quad (20a)$$

which, in view of (2), can be rewritten as

$$\hat{g}_i(t) = \frac{1}{2} \left\{ \left(\frac{v_{i+1}}{M_{i+1}} - \frac{v_i}{M_i} \right) \dot{r}_{i+1}(t) + \left(\frac{v_{i-1}}{M_{i-1}} - \frac{v_i}{M_i} \right) \dot{r}_{i-1}(t) - \frac{F_c^{i+1}(t)}{M_{i+1}} - \frac{F_c^{i-1}(t)}{M_{i-1}} \right\}. \quad (20b)$$

Here, we may consider the navigation strategy given by (14) with $g_i(t)$ replaced by $\hat{g}_i(t)$. If we use (20a) for $\hat{g}_i(t)$, the implementation of this strategy requires a knowledge of the accelerations of the neighboring robots. Alternatively, we could use (20b) for $\hat{g}_i(t)$. The implementation of this navigation strategy requires a knowledge of the velocities and control forces of the neighboring robots. Since both $F_c^{i+1}(t)$ and $F_c^{i-1}(t)$ depend on $\hat{g}_i(t)$ for $2 < i < N-1$, it is impossible to obtain an explicit expression for $\hat{g}_i(t)$. This difficulty can be alleviated by neglecting the terms involving $F_c^{i+1}(t)$ and $F_c^{i-1}(t)$ in (20b). In more general situations, we may take $d_i(t)$ to be the barycenter of k neighbors of the i -th robot at time t . For a fleet of identical robots, a follower robot with the foregoing strategy tries to maintain equal distance from its neighbors at all times, thus reducing the possibility of collisions.

3.3 Inertially Referenced Movements: Here, the formation pattern $\mathcal{P}(t)$ is generated by assigning a desired motion $\{\tilde{d}_i(t); t \in \bar{I}_T\}$ relative to the inertial frame for each robot. As in the previous case, we require that $\|\tilde{d}_i(t)$

$-\tilde{d}_{i-1}(t)\| > \rho_i + \rho_{i-1}$ for all $t \in \bar{I}_T$ so as to avoid the possibility of collisions between the i -th and $(i-1)$ -th robots. Thus, each robot tries to navigate along its own desired trajectory without any knowledge of the motions of the remaining robots in the fleet. A simple navigation strategy for this case is given by (14) with $E_i(t)$ and $g_i(t)$ replaced respectively by

$$\tilde{E}_i(t) \triangleq \tilde{d}_i(t) - r_i(t), \quad \tilde{g}_i(t) \triangleq \ddot{\tilde{d}}_i(t) + v_i M_i^{-1} \dot{\tilde{d}}_i(t), \quad i = 1, \dots, N. \quad (21)$$

3.4 Mixed Nearest-Neighbor Tracking and Inertially Referenced Movements: In nearest-neighbor tracking, it is assumed that the information on the position, velocity and navigation strategy of the previous neighbor is available at all times. For a mobile robot whose vision system has limited range of visibility, it is possible that the previous neighbor is temporarily invisible due to large tracking error, and it is impossible to determine the relative position and velocity by means of its vision system. Assuming that communication between robots is not permissible but the nominal desired motion of each robot with respect to an inertial frame is known, then the robot may navigate using the inertially referenced information. In this case, we have a mixture of the strategies described in Sections 3.1 and 3.3.

4. FORMATION PATTERN STABILITY

Suppose we are given a fleet of N mobile robots each having its own navigation strategy and desired motion d_i

$= d_i(t)$ defined for $t \geq 0$ such that $\{d_i(t), i = 1, \dots, N\}$ generates a desired formation pattern $\mathcal{P}(t)$ for each t . We introduce an error measure $\Delta(t)$ for the robot fleet with respect to $\mathcal{P}(t)$ as follows:

$$\Delta(t) = \left[\sum_{i=1}^N \{ \gamma_{1i} \|E_i(t)\|^2 + \gamma_{2i} \|\dot{E}_i(t)\|^2 \} \right]^{1/2} \quad (22)$$

where γ_{1i} and γ_{2i} are specified positive weighting coefficients. In the case where the formation is generated by nearest-neighbor tracking as discussed in Sec. 3.1, the summation in (22) is taken over the follower robots only. Now, we introduce the following definitions:

Def. A given desired formation pattern $\mathcal{P} = \mathcal{P}(t), t \geq 0$ for the robot fleet is said to be stable, if given any real number $\epsilon > 0$, there exists a $\delta > 0$ such that

$$\| (E(0), \dot{E}(0)) \| < \delta \Rightarrow \Delta(t) < \epsilon \quad \text{for all } t \geq 0, \quad (23)$$

where $E = (E_1, \dots, E_N) \in \mathbb{R}^{3N}$ and $\dot{E} = (\dot{E}_1, \dots, \dot{E}_N) \in \mathbb{R}^{3N}$. If in addition to (23), $\Delta(t) \rightarrow 0$ as $t \rightarrow \infty$, then the desired formation pattern $\mathcal{P} = \mathcal{P}(t), t \geq 0$ is said to be asymptotically stable.

In what follows, we shall derive a sufficient condition for asymptotic stability of a desired formation pattern for the case where the navigation strategies are based on nearest-neighbor tracking as discussed in Sec. 3.1. First, we shall show that under certain conditions depending on the robot's parameters, the tracking error $E_i(t)$ governed by (17) tends to 0 as $t \rightarrow \infty$. This task will be accomplished by considering the nature of the vector field defined by (17) in the (E_i, \dot{E}_i) -space.

First, we observe that (17) corresponds to a set of time-varying nonlinear differential equations of the form:

$$\begin{aligned} M_1 \ddot{e}_{1j} + \nu_1 \dot{e}_{1j} &= M_1 g_{1j}(t) - \bar{F}_c^{-1} \text{Sat}\{(M_1 g_{1j}(t) \\ &+ K_{11} e_{1j} + K_{12} \dot{e}_{1j}) / \bar{F}_c\}, \quad i = 2, \dots, N, \quad j = x, y, z, \quad (24) \end{aligned}$$

where e_{1j} and g_{1j} denote the j -th components of E_1 and g_1 respectively. Since $g_{1j}(t)$ depends only on $r_{i-1}(t), \bar{F}_c^{-1}(t)$ and $q_1(t)$, it can be regarded as a known input to (24). Clearly, the origin $0 \in \mathbb{R}^6$ is the unique equilibrium state of (24) if and only if the components of $g_1(t)$ satisfy

$$|g_{1j}(t)| \leq \bar{F}_c^{-1} M_1, \quad j = x, y, z \quad \text{for all } t. \quad (25)$$

In what follows, we shall derive a sufficient condition for the asymptotic stability of the desired formation pattern by requiring the origin of (24) to be asymptotically stable in the sense of Lyapunov for each i starting with $i = 2$.

First, we require that the trajectories of (24) near the origin be nonoscillatory. This can be attained by setting $\omega_1^2 \triangleq K_{11}/M_1 > 0$, and

$$\zeta_1 \triangleq (\nu_1 + K_{12}) / (2\omega_1 M_1) > 1 \quad (26)$$

so that the linearized system about the origin of \mathbb{R}^2 corresponding to (24) has negative real eigenvalues given by

$$\lambda_{11} = -\zeta_1 + (\zeta_1^2 - 1)^{1/2}, \quad \lambda_{12} = -\zeta_1 - (\zeta_1^2 - 1)^{1/2}. \quad (27)$$

The subspaces spanned by the eigenvectors corresponding to λ_{11} and λ_{12} are given by

$$\begin{aligned} S_{11} &= \text{Span} [1, \{-\zeta_1 + (\zeta_1^2 - 1)^{1/2}\} \omega_1]^T, \\ S_{12} &= \text{Span} [1, \{-\zeta_1 - (\zeta_1^2 - 1)^{1/2}\} \omega_1]^T. \end{aligned} \quad (28)$$

Since the equations for the tracking errors of the follower robots have the same form (24), we shall drop the super and subscripts i for robot identification in the subsequent development to simplify the notations.

Let $\mathcal{A}_j(t)$ be the intersection of the negative half-spaces $H_k^j(t)$, $k = R, L, T$ and B defined by

$$\begin{aligned} H_R^j(t) &= \{w_j \in \mathbb{R}^2: \langle K, w_j \rangle \leq \bar{F}_c - Mg_j(t)\}, \\ H_L^j(t) &= \{w_j \in \mathbb{R}^2: \langle K, w_j \rangle \leq -\bar{F}_c - Mg_j(t)\}, \\ H_T^j(t) &= \{w_j \in \mathbb{R}^2: \dot{e}_j \leq \dot{e}_j^+(t)\}, \\ H_B^j(t) &= \{w_j \in \mathbb{R}^2: \dot{e}_j \geq \dot{e}_j^-(t)\}, \end{aligned} \quad (29)$$

where $w_j = (e_j, \dot{e}_j)^T$; $K = (K_1, K_2)^T$. The velocities $\dot{e}_j^+(t)$ and $\dot{e}_j^-(t)$ are determined by the intersection of S_{11} and the lines $L_1^j(t) = \{w_j \in \mathbb{R}^2: \langle K, w_j \rangle = \bar{F}_c - Mg_j(t)\}$ and $L_2^j(t) = \{w_j \in \mathbb{R}^2: \langle K, w_j \rangle = -\bar{F}_c - Mg_j(t)\}$ respectively. They are given explicitly by

$$\begin{aligned} \dot{e}_j^+(t) &\triangleq -\alpha(\bar{F}_c + Mg_j(t)) / (\alpha K_2 + K_1) > 0, \\ \dot{e}_j^-(t) &\triangleq \alpha(\bar{F}_c - Mg_j(t)) / (\alpha K_2 + K_1) < 0, \end{aligned} \quad (30)$$

provided that

$$K_1 + \alpha K_2 > 0, \quad (31)$$

where α denotes the slope of the line corresponding to the subspace S_{11} given by

$$\alpha \triangleq -\{\nu + K_2 - ((\nu + K_2)^2 - 4K_1 M)^{1/2}\} / (2M) < 0. \quad (32)$$

It can be readily verified that (31) is satisfied if and only if

$$K_1/K_2 < \nu/M. \quad (33)$$

Moreover, if

$$K_2 \neq \nu, \quad (34)$$

then $\nu + K_2 > 2(\nu K_2)^{1/2}$ for positive ν and K_2 , and (33) implies condition (26). A sketch of $\mathcal{A}_j(t)$ is given in Fig. 3.

Let $f_j = f_j(t, w_j)$ denote the vector field on \mathbb{R}^2 at time t corresponding to (24) given by

$$\begin{aligned} f_j(t, w_j) &= [\dot{e}_j, g_j(t) - \bar{F}_c M_1^{-1} \text{Sat}(Mg_j(t) \\ &+ \langle K, w_j \rangle) - \nu M_1^{-1} \dot{e}_j]^T. \end{aligned} \quad (35)$$

The inner product of the vector field $f_j(t, w_j)$ with an outward normal at a point on the boundary face $\mathcal{F}_{jk}(t)$ of $\mathcal{A}_j(t)$ (see Fig. 3) is given by

$$\begin{aligned} \langle K, f_j(t, w_j) \rangle &= K_2 M^{-1} (Mg_j(t) - \bar{F}_c) \\ &+ K_2 (K_1 K_2^{-1} - \nu M^{-1}) \dot{e}_j \quad \text{on } \mathcal{F}_{jR}(t), \end{aligned} \quad (36a)$$

$$\begin{aligned} \langle K, f_j(t, w_j) \rangle &= -K_2 M^{-1} (Mg_j(t) + \bar{F}_c) \\ &- K_2 (K_1 K_2^{-1} - \nu M^{-1}) \dot{e}_j \quad \text{on } \mathcal{F}_{jL}(t), \end{aligned} \quad (36b)$$

$$\langle (0,1)^T, f_j(t, w_j) \rangle = -M^{-1} \{ (K_2 + \nu) \dot{e}_j + K_1 e_j \} \text{ on } \mathcal{F}_{jT}(t), \quad (36c)$$

$$\langle (0,-1)^T, f_j(t, w_j) \rangle = M^{-1} \{ (K_2 + \nu) \dot{e}_j + K_1 e_j \} \text{ on } \mathcal{F}_{jB}(t). \quad (36d)$$

The inner products given by (36a) and (36b) are nonpositive if

$$(K_1 K_2^{-1} - \nu M^{-1}) \dot{e}_j \leq \bar{F}_c M^{-1} - g_j(t), \quad (37)$$

and

$$-(K_1 K_2^{-1} - \nu M^{-1}) \dot{e}_j \leq \bar{F}_c M^{-1} + g_j(t) \quad (38)$$

are satisfied respectively. It can be verified that under conditions (25) and (33), $\dot{e}_j^+(t)$ and $\dot{e}_j^-(t)$ given by (30) satisfy (37) and (38) respectively. Thus, the inner products given by (36a) and (36b) are both nonpositive. Using (30), we obtain

$$\begin{aligned} \mathcal{F}_{jT}(t) &= \{ (e_j, \dot{e}_j) : -(\bar{F}_c + Mg_j(t)) / (K_1 + \alpha K_2) \leq e_j \\ &\leq K^{-1} [\bar{F}_c - Mg_j(t) + \alpha K_2 (\bar{F}_c + Mg_j(t)) (K_1 + \alpha K_2)^{-1}], \\ &\dot{e}_j = \dot{e}_j^+ \}. \end{aligned} \quad (39)$$

$$\begin{aligned} \mathcal{F}_{jB}(t) &= \{ (e_j, \dot{e}_j) : -K_1^{-1} [\bar{F}_c + Mg_j(t) \\ &+ K_2 \alpha (\bar{F}_c - Mg_j(t)) (K_1 + \alpha K_2)^{-1}] \leq e_j \\ &\leq (\bar{F}_c - Mg_j(t)) / (K_1 + \alpha K_2), \dot{e}_j = \dot{e}_j^- \}. \end{aligned} \quad (40)$$

By direct computation, we can verify that under conditions (25), (33) and (34), the inner products given by (36c) and (36d) are also nonpositive. Thus, under conditions (25), (33) and (34), the vector field $f_j(t, \cdot)$ at any point on the boundary $\partial \mathcal{A}_j(t)$ of $\mathcal{A}_j(t)$ is directed toward the interior of $\mathcal{A}_j(t)$ or tangent to $\partial \mathcal{A}_j(t)$ for every $t \geq 0$. In the strip $\mathcal{S}_j(t) = H_R^j(t) \cap H_L^j(t)$ containing $\mathcal{A}_j(t)$, the vector field defined by $f_j(e_j, \dot{e}_j) = [\dot{e}_j, -(\nu + K_2)M^{-1}\dot{e}_j - K_1 M^{-1}e_j]^T$ corresponding to (13) is time-invariant, and under conditions (25), (33) and (34), the origin $(e_j, \dot{e}_j) = (0,0)$ is a stable node in the interior of $\mathcal{A}_j(t)$. From (24), we deduce the following properties of the vector field f_j outside the strip $\mathcal{S}_j(t)$ (see Fig.3):

For $(e_j, \dot{e}_j) \in R^2 \setminus H_R^j$:

$$\frac{de_j}{de_j} = \frac{\nu}{M} + \frac{(g_j(t) - \bar{F}_c M^{-1})}{\dot{e}_j} \begin{cases} > 0 \text{ if } (Mg_j(t) - \bar{F}_c) / \nu < \dot{e}_j < 0, \\ = 0 \text{ if } \dot{e}_j = (Mg_j(t) - \bar{F}_c) / \nu, \\ = -\infty \text{ if } \dot{e}_j = 0, \\ < 0 \text{ if } \dot{e}_j > 0 \text{ or } \dot{e}_j < (Mg_j(t) - \bar{F}_c) / \nu; \end{cases} \quad (41)$$

and for $(e_j, \dot{e}_j) \in R^2 \setminus H_L^j$:

$$\frac{de_j}{de_j} = \frac{\nu}{M} + \frac{(g_j(t) + \bar{F}_c M^{-1})}{\dot{e}_j} \begin{cases} > 0 \text{ if } \dot{e}_j < 0 \text{ or } \dot{e}_j > (Mg_j(t) + \bar{F}_c) / \nu, \\ = 0 \text{ if } \dot{e}_j = (Mg_j(t) + \bar{F}_c) / \nu, \\ = +\infty \text{ if } \dot{e}_j = 0, \\ < 0 \text{ if } 0 < \dot{e}_j < (Mg_j(t) + \bar{F}_c) / \nu. \end{cases} \quad (42)$$

We observe that as $g_j(t)$ varies with time, the boundary of the strip $\mathcal{S}_j(t)$ shifts along the e_j -axis, and

all the trajectories initiated outside the strip at time $t=0$ are attracted to $\mathcal{S}_j(t)$ as t increases from 0.

Moreover, all the trajectories initiated outside $\mathcal{A}_j(0)$ are attracted to $\mathcal{A}_j(t)$ as t increases from 0.

Consequently, under conditions (25), (33) and (34), all trajectories of (24) tend to the origin of R^6 as $t \rightarrow \infty$ implying that each follower robot approaches its desired motion as $t \rightarrow \infty$. This implies that the desired formation pattern is asymptotically stable.

Remark 1: The foregoing result is valid provided that collisions between robots do not occur during the course of motion. This is possible if the norm $\|E(0), \dot{E}(0)\|$ is sufficiently small and the norms of the deviation vectors $q_i(t)$ are sufficiently large.

Remark 2: Since conditions (25), (33) and (34) do not depend on the specific form of the desired formation pattern, the foregoing result is valid for the class of formation patterns such that their corresponding g_i^s satisfy condition (25).

The foregoing results are also applicable to the case of inertially referenced movements discussed in Sec.3.2 by replacing e_j and g_j by \tilde{e}_j and \tilde{g}_j respectively.

5. SIMULATION STUDY

The main objectives of the simulation study are to determine the dynamic behavior of a fleet of robots each equipped with the proposed navigation strategies for movements in formation based on nearest-neighbor or multi-neighbor tracking. We consider a fleet of three identical robots with parameters $M_1 = 1$, $\nu_1 = 0.5$ and $\bar{F}_c^1 = 1$, $i = 1, 2, 3$ (all in appropriate units) moving in the (x, y) -plane. For nearest-neighbor tracking, we let the first robot be the fleet leader. The feedback gains K_{i1} and K_{i2} , $i = 2, 3$, are set to 1 and 2.5 respectively so that $\zeta_1 = 1.5$ and the stability conditions (33) and (34) are satisfied.

First, we let the deviation vectors $q_i(t) = (1, 0)^T$, $i = 2, 3$. In this case, $g_i(t)$ defined by (10) reduces to $F_c^{i-1}(t)/M_i$. The control force for the first robot (fleet leader) is taken as $F_c^1(t) = (\cos t, \sin t)^T$, $t \geq 0$. Figure 4 shows the robot motion in the (x, y) -plane starting from the initial positions $(x_1(0), y_1(0)) = (1, 0)$, $(x_2(0), y_2(0)) = (3, 0)$ and $(x_3(0), y_3(0)) = (5, 0)$ at $t = 0$ with initial velocities $(\dot{x}_1(0), \dot{y}_1(0)) = (0, 1)$, $i = 1, 2, 3$. It can be seen that the robot motion tends to a formation such that the x and y coordinates of the robot positions are separated by 1 and 0 respectively as specified by $q_i(t)$. Now we exchange the initial positions of robots 2 and 3 as given in Fig.4. Figure 5 shows the robot motion for this case. Here, the second and third robots must exchange positions in order to attain the desired formation pattern. We observe that a collision between robots 2 and 3 occurs in the vicinity of point A. This is due to the fact that the second robot tries to track the leader without considering the motion of the third robot. Evidently, for the navigation strategy (14), collision-free motion is attainable only for certain sets of initial states of the robots. Figure 6 shows the robot motions for the case where the friction coefficient ν_1 of the first robot is reduced to 0.1 and the deviation vectors $q_i = (0, -1)^T$ for $i = 2, 3$.

Here, the i -th follower robot tries to move alongside the $(i-1)$ -th robot at a unit distance away in the y -direction. The robots are initially at rest with

positions $(x_1(0), y_1(0)) = (4, 0)$, $(x_2(0), y_2(0)) = (0, 2)$ and $(x_3(0), y_3(0)) = (0, 0)$. It can be seen from Fig. 6 that the robot motion tends to the desired formation pattern with increasing t . Next, we consider the case where both the second and third robots try to follow the leader with deviation vectors $q_2 = (-1, -1)^T$ and $q_3 = (1, -1)^T$ respectively. Here, the desired formation pattern at any fixed time is a triangle. The robot parameters are identical to those corresponding to Fig. 6. Figure 7 shows the robot motion for this case with all robots starting from rest with initial positions $(x_1(0), y_1(0)) = (0, 0)$, $(x_2(0), y_2(0)) = (-2, 0)$ and $(x_3(0), y_3(0)) = (2, 0)$.

Now we consider a fleet of three robots in which both the first and third robots are leaders whose control forces are given by $F_c^1(t) = (\cos t, \sin t)^T$ and $F_c^3(t) = (-\cos t, \sin t)^T$ respectively. The second follower robot adopts the navigation strategy given by (14) with $g_1(t)$ replaced by $\hat{g}_1(t)$ as defined by (20b), and with $d_1(t)$ defined by (18). Here we assume that the second robot has full knowledge of the control forces of both leaders. Figure 8 shows the robot motion for this case with all robots starting from rest with initial positions $(x_1(0), y_1(0)) = (0, 0)$, $(x_2(0), y_2(0)) = (1.7, 0)$ and $(x_3(0), y_3(0)) = (4, 0)$. It can be seen that the trajectory of the second robot tends to the median of the positions of the leaders as t increases from 0.

Finally, we form a fleet of four robots by adding a follower robot to the previous fleet, and assigning the first and fourth robots as leaders. In this case, the navigation strategies for the follower robots given by (14) with $g_1(t)$ replaced by $\hat{g}_1(t)$ as defined by (20b), and $d_1(t)$ defined by (18) cannot be obtained in explicit forms. Here, we assume that follower robots receive no information pertaining to the control forces of their neighbors. The robot motion for this case with all robots starting from rest with initial positions $(x_1(0), y_1(0)) = (0, 0)$, $(x_2(0), y_2(0)) = (2, 0)$, $(x_3(0), y_3(0)) = (4, 0)$ and $(x_4(0), y_4(0)) = (6, 0)$ is shown in Fig. 9.

Although the trajectories of the follower robots in the world space remain in a region bounded by those of the two leaders, their trajectory points are not equally spaced between the leaders' trajectory points as desired.

6. CONCLUDING REMARKS

In this paper, we have considered a few simple navigation strategies for mobile robots moving in formation. These strategies have features similar to those used by humans in steering land vehicles and aircraft in formation. Simulation results showed that the strategies based on nearest-neighbor tracking are effective when inter-robot communication and complete visibility of the neighboring robots are maintained at all times. In the simulation study, we have not incorporate any collision-avoidance strategies such as those given in [1] and [2] with the strategies for moving in formation derived here. Their incorporation would complicate considerably the interaction dynamics of the robots.

ACKNOWLEDGMENTS

This work was supported by the National Science Foundation Grant ECS 87-18473 and the Jet Propulsion Laboratory, Pasadena, California.

REFERENCES

- [1] P.K.C.Wang, "Interaction Dynamics of Multiple Mobile Robots with Simple Navigation Strategies," *J. Robotic Systems*, Vol. 6, pp. 77-101, 1989.
- [2] P.K.C.Wang, "Dynamics of Interacting Multiple Autonomous Mobile Robots in Bounded Spatial Domains," UCLA Engr. Rpt. No. 88-30, October, 1988.
- [3] S.K.Kambhampati and L.S.Davis, "Multiresolution Path Planning for Mobile Robots," *IEEE J. Robotics Automat.* Vol. RA-2, pp. 135-145, 1986.
- [4] V.J.Lumelsky and A.A.Stepanov, "Dynamic Path Planning for a Mobile Automaton with Limited Information on the Environment," *IEEE Trans. Automat. Contr.*, Vol. AC-31, pp. 1058-1063, 1986.
- [5] C.E.Thorpe, "Path Relaxation: Path Planning for a Mobile Robot," *Proc. AAAI Conf.*, Aug. 1984.
- [6] R. Aggarwal and G. Leitmann, "Avoidance Control," *ASME J. Dynam. Syst., Meas. Contr.*, Vol. 103, pp. 69-70, 1981.

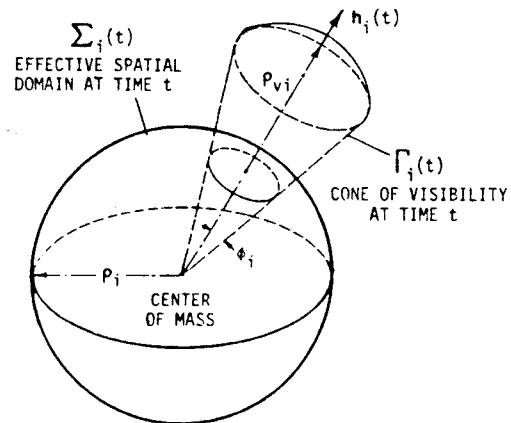


Fig. 1 Basic features of a mobile robot.

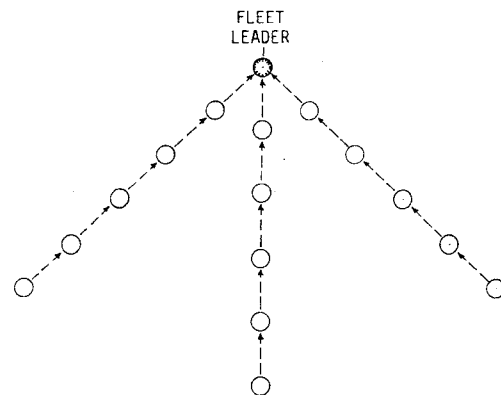


Fig. 2 Fleet formation pattern with multiple branches.

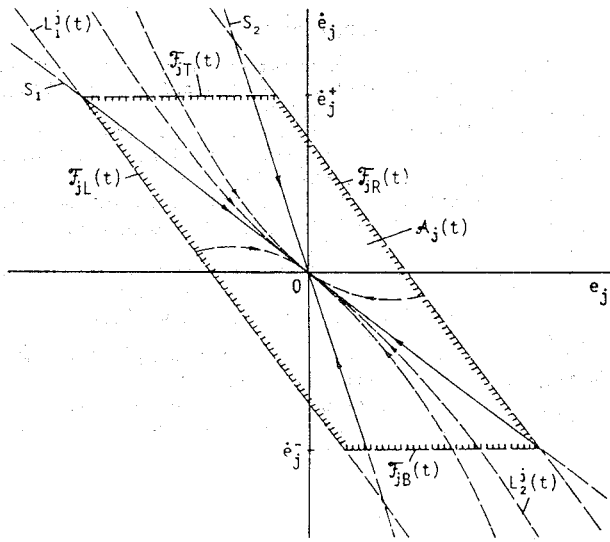


Fig. 3 Behavior of trajectories in the (e_j, \dot{e}_j) -plane.

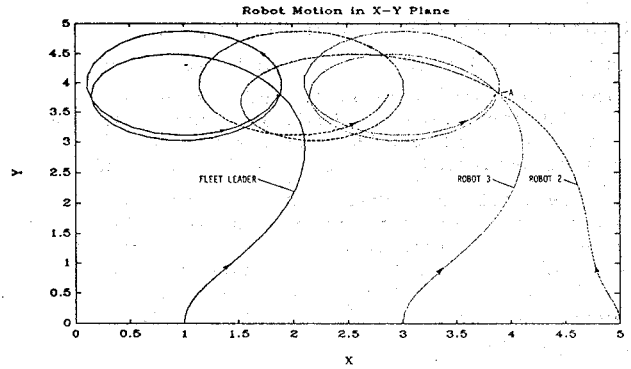


Fig. 5 Motion of a robot fleet with a single leader and nearest-neighbor tracking. Robot parameters (same as those in Fig. 4). Initial conditions: $(x_1(0), y_1(0)) = (1, 0)$, $(x_2(0), y_2(0)) = (5, 0)$, $(x_3(0), y_3(0)) = (3, 0)$; $(\dot{x}_1(0), \dot{y}_1(0)) = (0, 1)$, $i=1, 2, 3$.

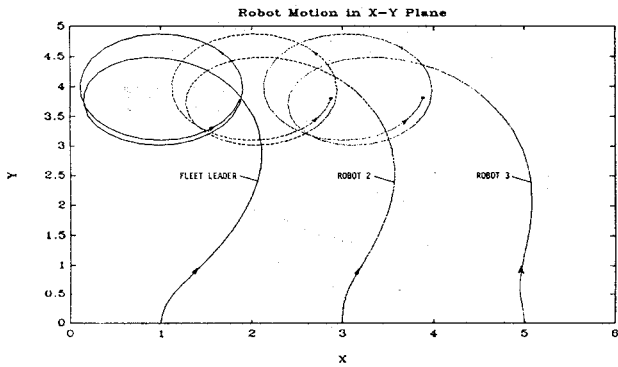
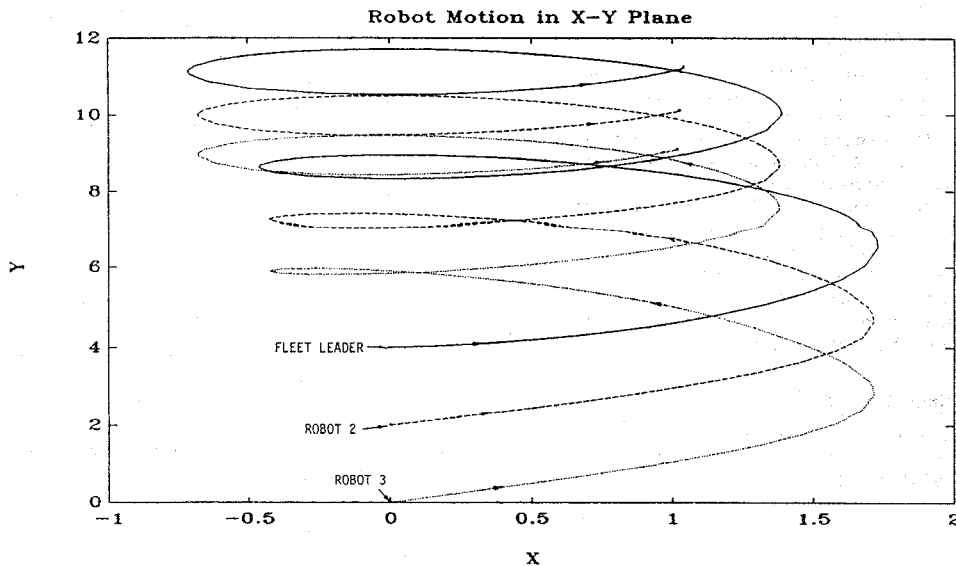


Fig. 4 Motion of a robot fleet with a single leader and nearest-neighbor tracking. Robot parameters: $M_i = 1$, $F_c^i = 1$, $v_i = 0.5$, $K_{i1} = 1$, $K_{i2} = 2.5$, $i = 1, 2, 3$.

Fig. 6 Motion of a robot fleet with a single leader and nearest-neighbor tracking. Robot parameters: $M_i = 1$, $F_c^i = 1$, $K_{i1} = 1$, $K_{i2} = 2.5$, $i = 1, 2, 3$; $v_1 = 0.1$, $v_2 = v_3 = 0.5$. Initial conditions: $(x_1(0), y_1(0)) = (0, 4)$, $(x_2(0), y_2(0)) = (0, 2)$; $(x_3(0), y_3(0)) = (0, 0)$; $(\dot{x}_i(0), \dot{y}_i(0)) = (0, 0)$, $i=1, 2, 3$.



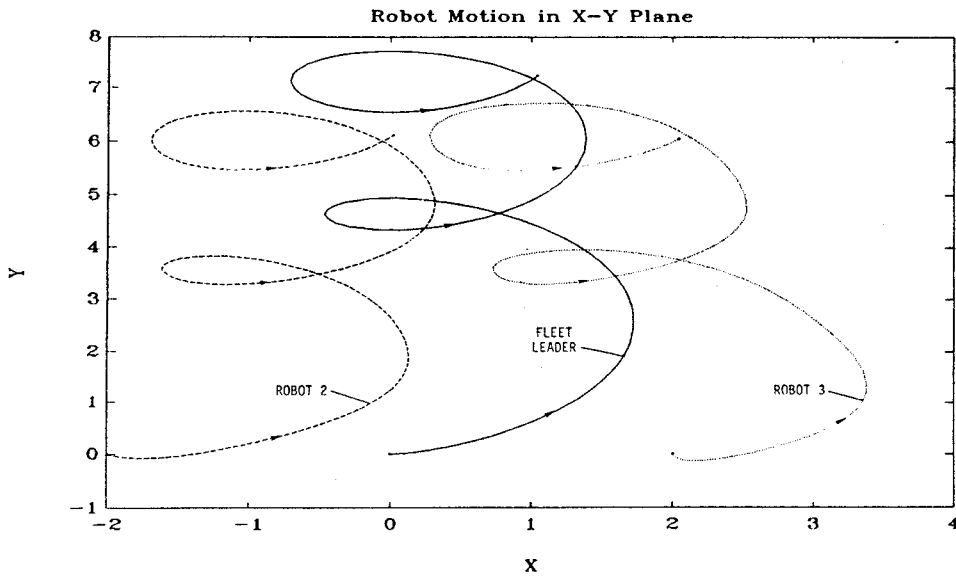


Fig.7 Motion of a robot fleet with two robots following a single leader. Robot parameters: $K_{i1}=1$, $K_{i2}=2.5$, $i=1,2,3$. $v_1=0.1$, $v_2=v_3=0.5$. Initial Conditions: $(x_1(0), y_1(0))=(0,0)$, $(x_2(0), y_2(0))=(-2,0)$, $(x_3(0), y_3(0))=(2,0)$; $(\dot{x}_i(0), \dot{y}_i(0))=(0,0)$, $i=1,2,3$.

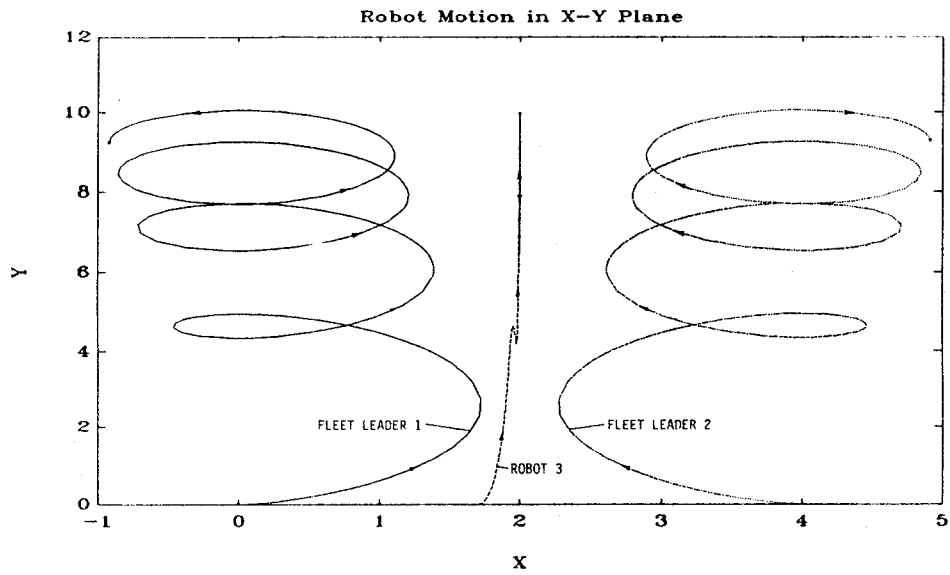


Fig.8 Motion of a robot fleet with two leaders and one follower. Robot Parameters (same as those in Fig.7): Initial conditions: $(x_1(0), y_1(0))=(0,0)$, $(x_2(0), y_2(0))=(1.7,0)$, $(x_3(0), y_3(0))=(4,0)$; $(\dot{x}_i(0), \dot{y}_i(0))=(0,0)$.

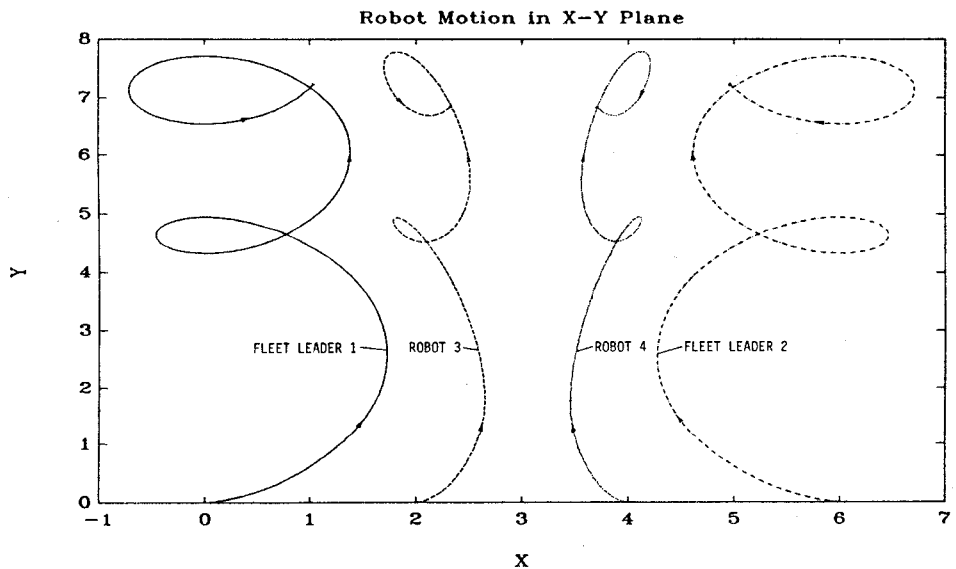


Fig.9 Motion of a robot fleet with two leaders and two followers. Robot parameters: $v_1=v_4=0.1$, $v_2=v_3=0.5$; $K_{i1}=1$, $K_{i2}=2.5$, $i=1,2,3$. Initial conditions: $(x_1(0), y_1(0))=(0,0)$, $(x_2(0), y_2(0))=(2,0)$, $(x_3(0), y_3(0))=(4,0)$, $(x_4(0), y_4(0))=(6,0)$; $(\dot{x}_i(0), \dot{y}_i(0))=(0,0)$, $i=1,2,3$.